Int j simul model 14 (2015) 4, 571-583
ISSN 1726-4529 Original scientific paper

COMPUTER VISION-BASED APPROACH TO END MILL TOOL MONITORING

Klancnik, S.; Ficko, M.; Balic, J. & Pahole, I.
University of Maribor, Faculty of Mechanical Engineering, Smetanova 17, 2000 Maribor, Slovenia
E-Mail: simon.klancnik@um.si, mirko.ficko@um.si, joze.balic@um.si, ivo.pahole@um.si

Abstract
The paper is concerned about the system of automatic detecting of wear and damages of the end mill tool by the use of computer vision. By using the algorithms developed for image segmentation and by an innovative approach to extraction of features describing individual end mill tool tooth the information representing significant features of the individual tool tooth is effectively gained from the captured image. The proposed approach to feature extraction is robust and independent of the scale and rotation of the end mill tool in the image. The features vectors have been classified by two approaches, i.e., *k*-nearest neighbour algorithm and artificial neural network. Both approaches have been tested by the test base of tool images and the results mutually compared. The classification has been validated by 10-fold cross-validation method. The best precision of classification (92.63 %) has been reached by the use of artificial neural network. Simulation results have confirmed that the proposed approach can improve monitoring of tool wear and damages and, consequently, the effectiveness and reliability of CNC milling machine tool.
(Received in August 2014, accepted in May 2015. This paper was with the authors 1 month for 1 revision.)

Key Words: Manufacturing System, Computer Vision, Machine Vision, *k*-Nearest Neighbours, End Mill Tool, Neural Network

1. INTRODUCTION

In modern production systems, computer vision is used as a substitute for human visual perception. The computer vision systems in production allow repeatability of processes, reduce production costs, improve product quality, guarantee human safety and reduce harmful effects of production process on environment. In production processes the computer vision is frequently used for product quality control, for controlling of technological processes, robot control, laboratory analyses of images etc. Monitoring of tool wear on CNC machine tools allows higher effectiveness of machines. In the cutting processes the tool may wear off or even be damaged. Therefore, it is very important that the control is enough frequent. Many researches deal with developing the approaches automatically, i.e. without human visual control, recognizing the tool condition. Those approaches include two principal spheres, i.e. direct and indirect methods [1]. Indirect measuring methods measure the extent of tool wear and damages by the use of sensors generating a signal indirectly representing the tool condition information. One of such approaches has been developed by Wang et al. [2], i.e. the tool condition monitoring system based on measuring vibrations of the machine tool. By the use of the support vector machine algorithm they, then, classified the measured vibrations and, consequentially, the tools into classes. Moradi et al. [3] dealt with thorough analysis of vibrations, primary and super-harmonic resonance and effects of tool wear on their changing. In the sphere of indirect tool monitoring methods, the researches, in the past, dealt a great deal with measuring the cutting forces and classifying the tool wear and damages on the basis of their changing [4-7]. In those works the researchers measure the cutting forces during machining and on their basis, with various deterministic approaches and with the use of intelligent methods; they classify the tool condition according to the features gained from measured cutting forces. The researches are also concerned about the indirect approach to tool monitoring on the basis of the noise captured by the use of microphone, while the signal is

properly processed and classified [8-10]. In case of direct methods, the tool monitoring is effected by means of optical systems and by the use of computer vision. In that sphere, the researchers, in the past, dealt with analyzing the texture of microscopic images of the material already machined and with classifying the extent of tool wear on the basis of data thus gained [11-14]. By that approach the tool wear or damages can be determined, when a specific material removal has already been performed. Alternatively, some researches are oriented towards direct optical control of the tool on the machine. In that case, by means of camera, the tool image is captured from which advanced image processing algorithms extract the information representing actual tool condition, while on the basis of the information the tool condition can be classified [15-17]. Additionaly, many researchers deal with developing models for predicting output responses such as tool wear based on cutting parameters [18-24].

In this paper we propose a new and effective approach to detection of the flank wear and damages of the end mill tool part by direct optical control. We have developed a robust procedure extracting from captured image the features appertaining to individual tool tooth. Effectiveness of the developed procedure and quality of extracted features are independent of the tool to camera distance, while capturing the image; consequentially the end mill tool diameter does not affect the system operation effectiveness. Further, when developing the system, we managed to reach an important property, i.e., that the system operation is independent of the tool rotation angle round its axis during image capturing, which is important for the use of the optical system on the machine tool. Within the research we performed classification of feature vectors by *k*-nearest neighbours (*k*-NN) approach and by the use of artificial neural network (ANN). The results of classification effectiveness by individual method were validated by 10-fold cross validation test and mutually compared.

The article is organized as follows: section 2 presents the basic concept of the proposed system and detailed description of individual components. The system test results with test base of captured images of tool and discussion are given in section 3. The article ends with a short conclusion.

2. METHODOLOGY AND SYSTEM COMPONENTS

Before machining, after machining and, if necessary, also during machining the tool of the CNC milling machine tool is moved into the predetermined position, where the image of the tool face part is captured by camera. Fixed position of camera and known tool location during the image capturing allows the tool to be placed always at right angle to the image plane. In that way, the effectiveness of the proposed system is increased. The process of the tool image capturing is shown in Fig. 1.

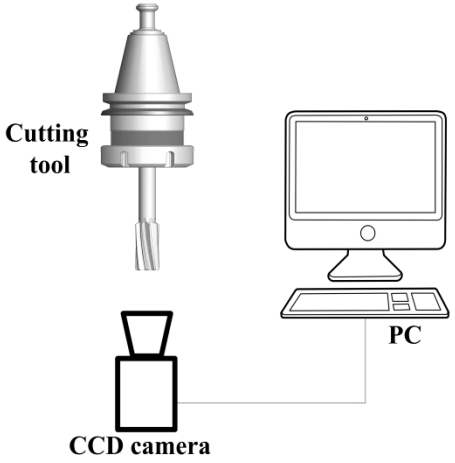

Figure 1: Computer vision-based tool monitoring system.

Fig. 2 shows functioning of the developed approach, where the image of the tool face part on the machine is captured by means of camera.

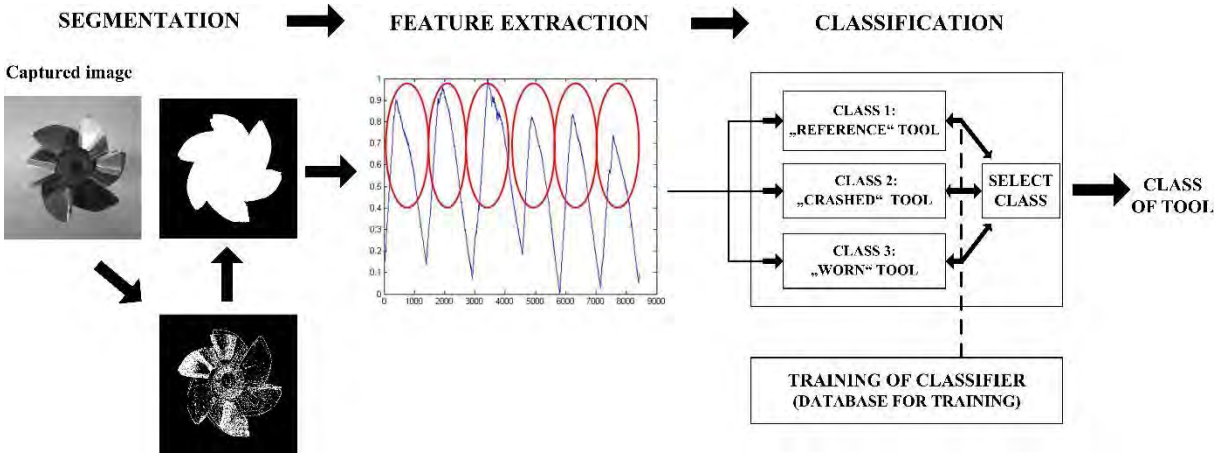

Figure 2: Computer vision-based approach for wear of end mill tool classification.

2.1 Segmentation

The tool must be detected in the captured image. Another term for detection of objects in the image is the segmentation. Image segmentation is typically used to locate objects and boundaries (lines, curves etc) in images. The result of the segmentation process is a set of segments covering together the entire image or a set of contours extracted from the image. All pixels in the segment have in common a certain property, for example color, intensity or texture. The developed segmentation process is schematically shown in Fig. 3.

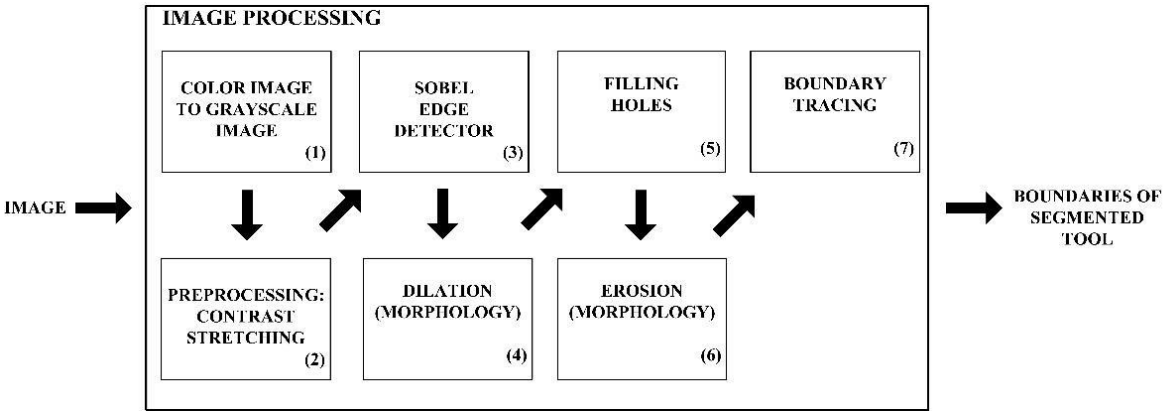

Figure 3: Object segmentation.

Herebelow, individual steps from Fig. 3 will be described in detail.

(1) Convert color image to Grayscale

The captured color image consists of basic colors: red, green and blue. The color image is first to be converted to 256-level grayscale. The value 0 of the picture element represents the black color in the image and the value 255 of the picture element the white color in the image. The process of color image conversion to grayscale is performed by weighting individual color channels according to the following equation:

$$Y(x,y) = 0{,}21 \cdot R(x,y) + 0{,}71 \cdot G(x,y) + 0{,}071 \cdot B(x,y) \quad (1)$$

By Eq (1) one pixel of the color image is converted to grayscale pixel. The coefficients in Eq. (1) are so selected that their sum equals one.

(2) Contrast stretching

Pre-processing is aimed at improving the image quality and effectiveness of the process developed. The contrast stretching is a method improving the image contrast according to the range of intensity values. The normalization process transforms the grayscale image $I: \{\mathbb{X} \subseteq \mathbb{R}^n\} \rightarrow \{\text{Min}, \ldots, \text{Max}\}$ with grayscale values in the range (Min, Max) into a new grayscale image $I_N : \{\mathbb{X} \subseteq \mathbb{R}^n\} \rightarrow \{\text{newMin}, \ldots, \text{newMax}\}$ with grayscale values in the interval (newMin, newMax). The contrast stretching of the grayscale image was performed according to the Eq. (2):

$$I_N = (I - \text{Min}) \cdot \frac{\text{newMax} - \text{newMin}}{\text{Max} - \text{Min}} + \text{newMin} \tag{2}$$

Fig. 4 shows the preprocessing result of the captured tool image by the method of contrast stretching.

a) Grayscale image b) Contrast stretching image

Figure 4: Contrast stretching of captured image: a) grayscale image; b) contrast stretching image.

(3) Sobel operator

Boundary points in the image are represented as sudden changes of intensity of neighbouring pixels. The faster the transition in intensities of those points (gradient) the greater the probability that they are located at the boundary. The change rate in intensities is obtained by calculating the differential function. As the image is a two-dimensional field of points, the two approximations of gradients of boundaries in directions x (G_x) and y (G_y) must be calculated by using partial differential functions. The approximations of those differential functions in the bit image can be obtained by applying two convolution masks. In our research, the Sobel operator was used for detection of boundaries. The Sobel detector uses two convolution masks of size 3×3 shown in Fig. 5 [25].

$G_x =$

1	0	-1
2	0	-2
1	0	-1

$G_y =$

1	2	1
0	0	0
-1	-2	-1

Figure 5: Sobel operator convolution masks.

In the end, the obtained values of both gradients (differential functions) are combined in order to obtain the absolute intensity of gradient. For faster calculating simply the approximation was used:

$$g(x, y) = |G_x| + |G_y| \tag{3}$$

If the value $g(x, y)$ exceeds a predetermined sill, then a boundary is at that place. The results of processing of the captured tool image by Sobel operator is shown in Fig. 6 a.

(4) Dilation

Dilation is one of the most frequently used operations of mathematical morphology [25, 26].

We used the dilation in order to increase gradually the limit of areas among the pixels themselves. Such areas grow, while the holes become smaller. Dilation is defined as:

$$A \oplus B = \bigcup_{x \in B} Ax \tag{4}$$

In Eq. (4) A represents the input image processed with dilation process. The B operator represents the structuring element and the x operator represents the core coordinates. The output image depends very much on the shape and value of the using core. In our case the 3×3 structuring element with values 1 was used. Fig. 6 b represents the result after processing by the dilation method.

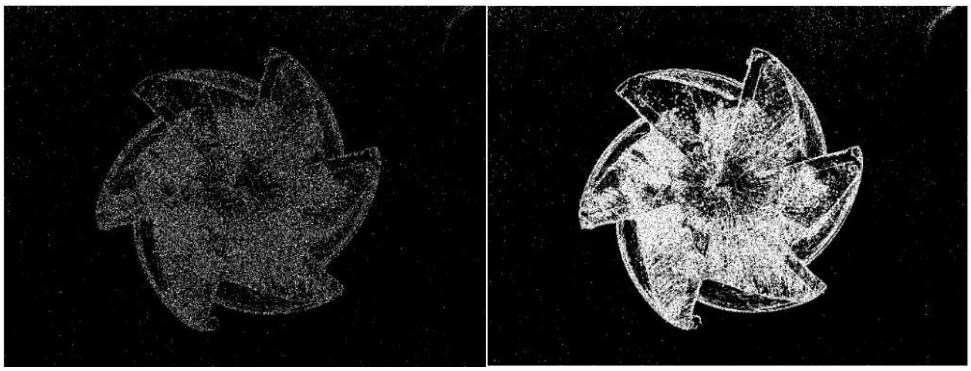

a) Sobel edge detection b) Image dilation

Figure 6: Results of Sobel edge detection (a) and dilation (b).

(5) Holes filling

The holes in the binary image are filled with values 1 at places, where the picture elements are closed according to the rule of 8-connected neighbourhood. The hole represents the image background limited with closed elements. The picture elements p and q with values 1 in the binary image are considered to be connected in terms of 8-connected neighbourhood, if q is the element of set $N_8(p)$ [25, 26]. The result of image processing by holes filling algorithm is shown in Fig. 8 a.

(6) Erosion

Erosion is a frequently used operation of mathematical morphology. The erosion process was used in order to reduce gradually the limit of areas between the picture elements themselves. Erosion is defined as:

$$A \ominus B = \{w : B_w \subseteq A\} \tag{5}$$

In Eq. (5) A represents the input image processed with erosion process. The B operator represents the structuring element and/or the core, while the w operator represents the structuring element coordinates. The result of the erosion operation mainly depends on the core shape and value. In our case, the diamond shape structural element with 13 neighbours shown in Fig. 7 was used.

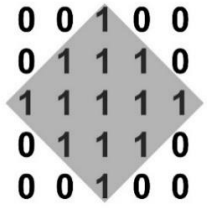

Figure 7: Diamond shape structural element.

For performance of erosion the core B is moved on the input image A and in that way all places are found, where A and B coincide. A relevant designation is assigned to all coincidence points; the set of all coincidence points forms the erosion. Fig. 8 b shows the result of image processing by erosion operation.

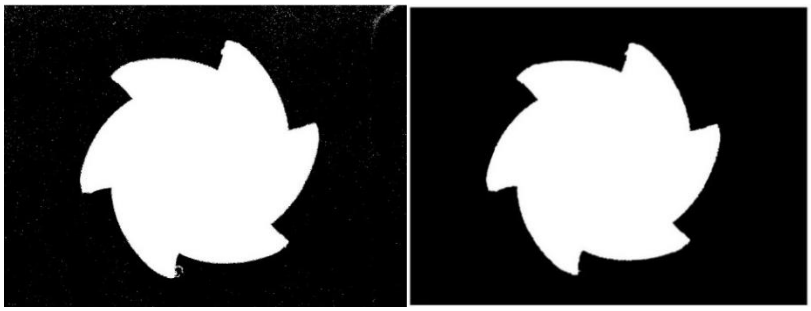

a) Holes filling b) Erosion

Figure 8: Results of filling holes (a) and erosion (b).

(7) Contour tracing

Contour tracing is the method used for determination of the object boundaries. The boundary detectors do not detect always the boundaries coinciding with actual boundaries in the image. Noise, spatial non-homogeneities and other disturbing factors cause interruption of detected boundaries. Therefore, in the last step of segmentation the image is processed by Moore-neighbour tracing algorithm [27]. The input information into the algorithm is the image I processed with all previously described steps. That image contains the connected points P representing the detected object. An example of the input binary image is shown in Fig. 8 b. The output from the algorithm is the set of points $T(t_1, t_2, \ldots, t_k)$ in 2D plane, representing the boundary of detected tool. For the contour tracing the Moore neighbourhood shown in Fig. 9 is used.

M(p) =

	$p1$	$p2$	$p3$	
	$p8$	p	$p4$	
	$p7$	$p6$	$p5$	

Figure 9: Moore Neighbourhood (also known as the 8-neighbours or indirect neighbours).

```
Let p denote the current boundary pixel.
Let c denote the current pixel under consideration i.e. c is in M(p).
Begin
Set T to be empty.
From bottom to top and left to right scan the cells of T until a black pixel, s, of P is found.
Insert s in T.
Set the current boundary point p to s i.e. p=s
Backtrack i.e. move to the pixel from which s was entered.
Set c to be the next clockwise pixel in M(p).
While c not equal to s do
  If c is black
      insert c in T
      set p=c
     backtrack (move the current pixel c to the pixel from which p was entered)
  else
 advance the current pixel c to the next clockwise pixel in M(p)
end While
End
```

Figure 10: Pseudocode of Moore Neighbourhood algorithm [27].

Fig. 10 shows the pseudocode of the used algorithm for contour tracing. The detected boundaries for the test image are shown in Fig. 11.

Figure 11: Results of contour tracing and centroid calculation.

2.2 Feature extraction

After segmentation of the captured image the detected object, i.e. in our case the tool must be properly described. Our principal aim was to develop an approach effectively reducing the quantity of data describing the object. We also wanted to develop an approach insensitive to location, rotation and scale of the object, as it is not possible on the machine tool to guarantee always identical conditions, when capturing the tool image.

In the first step the centroid of the segmented object in the image is calculated. The result of segmentation of the capture image is the binary image, where the values 1 represent the detected object and the values 0 the background. The centroid is calculated according to the equation:

$$\text{centroid}(g_x, g_y): \begin{cases} g_x = \frac{1}{N}\sum_{i=1}^{N} x_i \\ g_y = \frac{1}{N}\sum_{i=1}^{N} y_i \end{cases} \tag{6}$$

In Eq. (6) N stands for the number of points describing the object, $(x_i, y_i) \in \{(x_i, y_i) \mid f(x_i, y_i) = 1\}$.

An example of the calculated object centroid is shown in Figs. 11 and 12. By the segmentation process the object was detected and the points, representing boundaries of the detected object, calculated. Herebelow, the distances from centroid to each point ($x(t)$, $y(t)$) representing the object boundary points are calculated by equation:

$$r(t) = \sqrt{[(x(t) - g_x)^2 + (y(t) - g_y)^2]} \tag{7}$$

In Eq. (7) g_x and g_y represent the object centroid, while $x(t)$ and $y(t)$ represent the coordinates of points describing the detected object boundary points in the image.

Fig. 12 shows the tool description by the function of the distance of tool boundaries to centroid of the detected object. By normalization of calculate distances $r(t)$ it is guaranteed that the approach of the object feature description is independent of the object scale in the image and/or of the distance between the tool and camera, when capturing the image. The end mill tool can have different number of teeth.

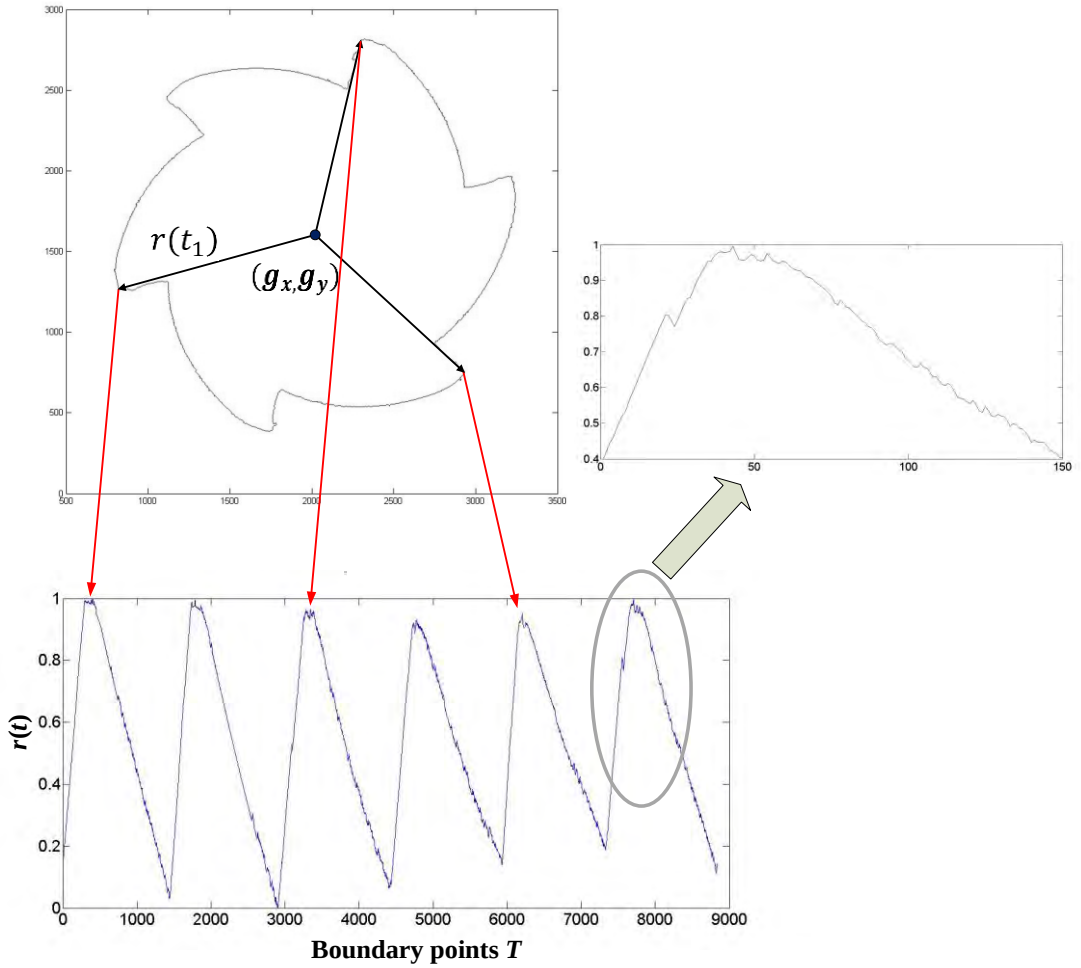

Figure 12: Tool description by the function of the distance of tool boundaries to centroid of the detected object.

In Fig. 8 b the end mill tool with six teeth is segmented. Our aim was to develop a system recognizing the wear and damages for each tooth on the tool separately. To that end, the tool features are divided into the interval so that each of intervals represents the features for individual tool tooth. Fig. 13 shows division of features for the end mill tool with six teeth.

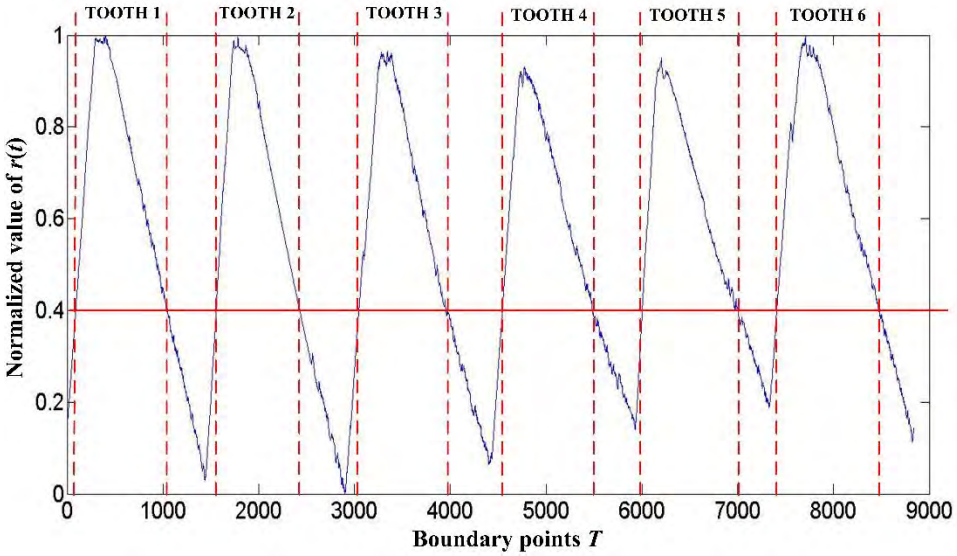

Figure 13: Determination of feature vector for each tooth separately.

The features for individual tool are determined by eliminating the distances $r(t)$ whose value is lower than 40 % value of maximum distance $r(t)$. In that way the graph of the function describing the features of the entire tool becomes discontinuous. When the value $r(t)$ has been reduced below 40 % of maximum distance $r(t)$, that implies the end of the features describing the tooth n. We have to move forwards on the abscissa axis of the graph in Fig. 13 and when the value $r(t)$ increases again above 40 % of maximum distance $r(t)$, that implies the beginning of features describing the cut n+1. That procedure is to be repeated through all boundary points.

The input vectors into the classifier must be of constant lengths; on the other hand, the great quantity of input data into classifier considerably extends the process of classification into classes. To that end, in the last step of data editing for classification, each interval representing the features for individual tool tooth is to be divided into 150 equal steps. Consequently the input vector of features for individual tool tooth consists of 150 distances $r(t)$ as shown at the right side of Fig. 12 for tooth 6.

2.3 Classification

By the process of classifications of features obtained from the captured tool image, the pre-defined category of individual tool tooth is determined. The features were divided into three classes according to the actual state of tools whose images had been captured. The class "Worn" was allotted to features representing worn tool tooth. Class "Crashed" was allotted to features representing damaged (broken) tool tooth, while class "Useful" was allotted to features representing the tool tooth which is not yet worn or damaged. For classification, two different classifiers were used, i.e., the *k*-nearest neighbour classifier and classification using artificial neural network.

K-nearest neighbours method belongs to numerical methods of machine learning. By that method practically there is no learning, therefore, it is said that it belongs to the category of lazy learning. If the class is to be predicted to a new sample, *k*-nearest neighbours are to be found among all training samples and, when classifying, the majority class, i.e. the class to which most *k*-nearest neighbours belong is to be predicted. The *k*-nearest neighbour method is a frequently used and well known method of machine learning.

The artificial neural networks belong to the methods of artificial intelligence. They are used for solving various problems, among other things for classification. In the research, the multilayer feed-forward neural network with back-propagation training algorithm was simulated (BP-ANN). The BP-ANN is constructed from the input layer of neurons, one or several hidden layers of neurons and output layer of neurons. In our research, the input layer was composed of 150 neurons, since that is dimension of the feature vector representing input into the BP-ANN. In the course of experiment, the number of hidden layers and the number of neurons in individual hidden layer was changed and optimum network topology searched for. The samples were classified into three classes; therefore the network topology was so conceived that the output layer was composed of three neurons. The feed-forward neural network is a frequently used and well known artificial intelligence method.

4. RESULTS AND DISCUSSION

Testing of the developed system was limited to end mill tools with six cutting tooth. The system is so conceived that it can be used for end mill tools with any number of cutting teeth, however, for each new geometry of tool the classifier must be trained with new training samples. For testing of the system 18 tool images with differently worn, broken or completely whole teeth were used. Each tool used had 6 cutting teeth so that 108 feature vectors were available in the base. Fig. 14 shows some images used in experiment. As already mentioned,

end mill tools with six cutting teeth and different diameters were used. The images were captured at different distances between camera and tool face part. Prior to each test image capturing the tool rotation round its axis was quite random; consequently the tool teeth were not aligned. Our aim was to confirm that functioning of the developed system was robust and quite independent of tool diameter, distance between tool and camera and angle of tool rotation round its axis, when capturing the image.

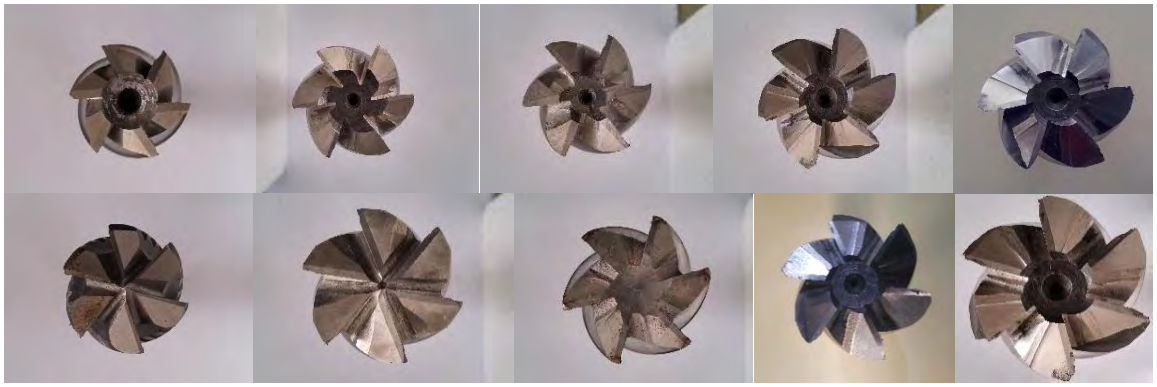

Figure 14: Sample images using in experiment.

Before execution of the tool teeth classification, efficient segmentation of the captured image is required, since that is to a great extent a prerequisite for successful classification. The results of segmentation of the tool test image from Fig. 4, which is one of the images used in experiment, are presented already in the preceding section for better presentation of algorithms, i.e. in Figs. 4, 6, 8 and 11. Results of feature extraction for that image are presented in Figs. 12 and 13.

On the basis of extracted features the developed system classifies each tooth into one of three classes. Classification includes the classes "Worn", "Crashed" and "Useful". Herebelow, the results of classification with the use of *k*-NN classifier and artificial neural network will be presented. For testing effectiveness of classifiers the experiment was performed in two steps. In the first step, the optimum control parameter of classifiers giving the least error of prediction in training and testing was selected. In that step the samples were divided into 90 % of training and 10 % of testing samples. In the second step of experiment the effectiveness of classification was verified still by the cross-validation method. Fig. 15 shows the feature classification accuracy with the use of *k*-NN classifier depending on the used number of neighbours *k*. The highest classification accuracy was reached with $k = 4$. In that case, the classifier classified accurately 12.04 % of training samples and 16.8 % of testing samples.

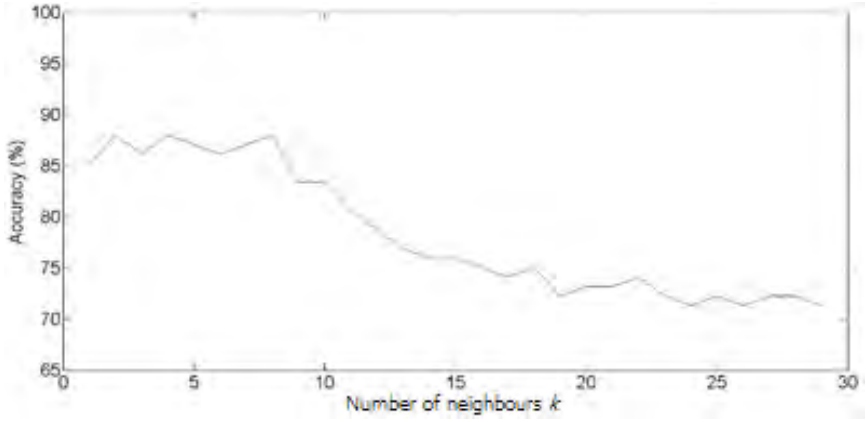

Figure 15: *k*-NN classification train accuracy according to number of neighbours *k*.

Table I shows the results of classification by the use of neural networks for different number of hidden layers and number of neurons in individual hidden layer of neural network. The best prediction accuracy for the test samples was reached with the use of neural network with three hidden layers, where there were 5 neurons in the first hidden layer, 10 neurons in the second hidden layer and again 5 neurons in the third hidden layer.

Table I: Results using feedforward neural network.

Exp#	Topology	Train accuracy (%)	Test accuracy (%)
1	150-10-3	89.47 %	68.75 %
2	150-20-3	92.10 %	75.11 %
3	150-5-5-3	90.79 %	68.83 %
4	150-10-10-3	100.00 %	68.75 %
5	150-20-20-3	100.00 %	75.10 %
6	**150-5-10-5-3**	**96.05 %**	**87.50 %**

Because of relatively low number of available samples for classification we decided to test classification still with the use of cross-validation which is very frequently used in technical literature for evaluation of effectiveness of sample classification. In cross-validation identical data are used for the classifier training and its validation. The number of folds m of specific data set was determined. The number of folds means the number of divisions of data set into subsets. In the continuation of the process the samples in the data set were mixed at random and divided into m of equally large subsets. After division the training process was started m-times. In each iteration, m-1 subsets of the data set were used for classifier training and the rest for its testing. 10-fold cross validation was used so that m was equal to $m = 10$. For the experiment we had available 108 samples, hence the validation process was performed 10 times; in each iteration 10 % of random samples representing the samples for classifier testing were selected. Table II shows the results of comparison of effectiveness of classification with k-NN and BP-ANN, verified by the 10 fold cross validation method. It can be seen that the BP-ANN method reached better effectiveness, since in the course of validation process it wrongly classified only 8 samples out of total 108 samples.

Table II: Comparison of the success rates of classifiers using 10-fold cross validation.

Method	Number of samples	Parameter	Number of misclassified samples	Success rates (%)
k-NN classifier	108	$k = 5$	15	86.11 %
BP-ANN classifier	108	Topology: 150-5-10-5-3	8	92.63 %

5. CONCLUSION

The paper presents a new approach to monitoring of end mill tools on CNC milling machine tool with the use of computer vision and machine learning. By developed algorithms the captured image is segmented and the features describing individual tool teeth in the image are extracted. The BP-ANN and k-NN algorithms are used to classify the detected tool teeth in the image into classes. Each tool tooth is classified into class “Worn”, “Crashed” or “Useful”. As stated in the paper, the simulation results with test base have shown that the proposed system establishes the tool wear and damages on CNC machines tool with acceptable accuracy. The research results represent a contribution in the sphere of tool condition monitoring in industrial environment.

With the use of the developed procedure of feature extraction from the capture image the information describing individual tool tooth condition is efficiently extracted. Besides, the developed approach acts so that the distance between camera and tool face part, when

capturing the image, does not affect the quality of features and, consequently, quality of classification. In the same way, the quality of features is not affected by different diameters of end mill tool and angle of tool rotation round its axis, when capturing the image. As a result, important properties giving proposed system a greater useful value for actual use on CNC machine tools have been attained. The research was limited to the use of two classifiers. Comparison of effectiveness of classification of worn, damaged and usable end-mill tools with *k*-NN and BP-ANN has shown that BP-ANN classifier gives better results.

As an extension to this study, we suggest research directions for the future work. It is possible to improve the segmentation process so that the tool detection in the captured image will be as robust and independent of disturbances as possible. In the research, for capturing the tool images we did not use additional object illumination which would guarantee more constant conditions. In the future, the tool segmentation effectiveness could be increased by integrating the light source onto the machine tool. Secondly, we propose extension of the system with additional camera covering the lateral part of the tool so that, in addition to wear and damages on the tool face part, it would detect also the changes on the tool side part. Thirdly, it would be rational to test functioning of the system still with other machine learning methods, such as Support vector machine, Naive-Bayes classifier, Decision trees, Boosting etc. and to perform their validation and comparison of classification accuracy.

REFERENCES

[1] Volkan Atli, A.; Urhan, O.; Erturk, S.; Sonmez, M. (2006). A computer vision-based fast approach to drilling tool condition monitoring, *Journal of Engineering Manufacture*, Vol. 220, No. 9, 1409-1415, doi:10.1243/09544054JEM412

[2] Wang, G. F.; Yang, Y. W.; Zhang, Y. C.; Xie, Q. L. (2014). Vibration sensor based tool condition monitoring using *v* support vector machine and locality preserving projection, *Sensors and Actuators A: Physical*, Vol. 209, 24-32, doi:10.1016/j.sna.2014.01.004

[3] Moradi, H.; Vossoughi, G.; Movahhedy, M. R.; Ahmadian, M. T. (2013). Forced vibration analysis of the milling process with structural nonlinearity, internal resonance, tool wear and process damping effects, *International Journal of Non-Linear Mechanics*, Vol. 54, 22-34, doi:10.1016/j.ijnonlinmec.2013.02.005

[4] Wang, G.; Yang, Y.; Xie, Q.; Zhang, Y. (2014). Force based tool wear monitoring system for milling process based on relevance vector machine, *Advances in Engineering Software*, Vol. 71, 46-51, doi:10.1016/j.advengsoft.2014.02.002

[5] Cus, F.; Milfelner, M.; Balic, J. (2006). An intelligent system for monitoring and optimization of ball-end milling process, *Journal of Materials Processing Technology*, Vol. 175, No. 1-3, 90-97, doi:10.1016/j.jmatprotec.2005.04.041

[6] Milfelner, M.; Kopac, J.; Cus, F.; Zuperl, U. (2005). Genetic equation for the cutting force in ball-end milling, *Journal of Materials Processing Technology*, Vol. 164-165, 1554-1560, doi:10.1016/j.jmatprotec.2005.02.147

[7] Cus, F.; Zuperl, U. (2015). Surface roughness control simulation of turning processes, *Strojniski vestnik – Journal of Mechanical Engineering*, Vol. 61, No. 4, 245-253, doi:10.5545/sv-jme.2014.2345

[8] Rafezi, H.; Akbari, J.; Behzad, M. (2012). Tool Condition Monitoring based on sound and vibration analysis and wavelet packet decomposition, *2012 8th International Symposium on Mechatronics and its Applications (ISMA)*, Sharjah, 1-4, doi:10.1109/ISMA.2012.6215170

[9] Quintana, G.; Ciurana, J.; Ferrer, I.; Rodríguez, C. A. (2009). Sound mapping for identification of stability lobe diagrams in milling processes, *International Journal of Machine Tools and Manufacture*, Vol. 49, No. 3-4, 203-211, doi:10.1016/j.ijmachtools.2008.11.008

[10] Salgado, D. R.; Alonso, F. J. (2007). An approach based on current and sound signals for in-process tool wear monitoring, *International Journal of Machine Tools and Manufacture*, Vol. 47, No. 14, 2140-2152, doi:10.1016/j.ijmachtools.2007.04.013

[11] Ramamoorthy, B.; Radhakrishnan, V. (1993). Statistical approaches to surface texture classification, *Wear*, Vol. 167, No. 2, 155-161, doi:10.1016/0043-1648(93)90320-L
[12] Kassim, A. A.; Mian, Z.; Mannan, M. A. (2004). Connectivity oriented fast Hough transform for tool wear monitoring, *Pattern Recognition*, Vol. 37, No. 9, 1925-1933, doi:10.1016/j.patcog.2004.01.014
[13] Kassim, A. A.; Mian, Z.; Mannan, M. A. (2002). Texture analysis using fractals for tool wear monitoring, *Proceedings of 2002 International Conference on Image processing*, Vol. 3, 105-108, doi:10.1109/ICIP.2002.1038915
[14] Bradley, C.; Wong, Y. S. (2001). Surface texture indicators of tool wear – A machine vision approach, *International Journal of Advanced Manufacturing Technology*, Vol. 17, No. 6, 435-443, doi:10.1007/s001700170161
[15] Pfeifer, T.; Wiegers, L. (2000). Reliable tool wear monitoring by optimized image and illumination control in machine vision, *Measurement*, Vol. 28, No. 3, 209-218, doi:10.1016/S0263-2241(00)00014-2
[16] Kerr, D.; Pengilley, J.; Garwood, R. (2006). Assessment and visualisation of machine tool wear using computer vision, *International Journal of Advanced Manufacturing Technology*, Vol. 28, No. 7-8, 781-791, doi:10.1007/s00170-004-2420-0
[17] Jurkovic, J.; Korosec, M.; Kopac, J. (2005). New approach in tool wear measuring technique using CCD vision system, *International Journal of Machine Tools & Manufacture*, Vol. 45, No. 9, 1023-1030, doi:10.1016/j.ijmachtools.2004.11.030
[18] Senthilkumar, N.; Tamizharasan, T.; Anandakrishnan, V. (2013). An ANN approach for predicting the cutting inserts performances of different geometries in hard turning, *Advances in Production Engineering & Management*, Vol. 8, No. 4, 231-241, doi:10.14743/apem2013.4.170
[19] Mgwatu, M. I. (2013). Integrated approach for optimising machining parameters, tool wear and surface quality in multi-pass turning operations, *Advances in Production Engineering & Management*, Vol. 8, No. 4, 209-218, doi:10.14743/apem2013.4.168
[20] Hrelja, M.; Klancnik, S.; Balic, J. & Brezocnik, M. (2014). Modelling of a turning process using the gravitational search algorithm, *International Journal of Simulation Modelling*, Vol. 13, No. 1, 30-41, doi:10.2507/IJSIMM13(1)3.248
[21] Chen, C.-H.; Wang, Y.-C.; Lee, B.-Y. (2013). The effect of surface roughness of end-mills on optimal cutting performance for high-speed machining, *Strojniski vestnik – Journal of Mechanical Engineering*, Vol. 59, No. 2, 124-134, doi:10.5545/sv-jme.2012.677
[22] Saric, T.; Simunovic, G.; Simunovic, K. (2013). Use of neural networks in prediction and simulation of steel surface roughness, *International Journal of Simulation Modelling*, Vol. 12, No. 4, 225-236, doi:10.2507/IJSIMM12(4)2.241
[23] Liu, C.; Wang, G.; Dargusch, M. S. (2014). Mechanics and dynamics of helical milling operations, *Strojniski vestnik – Journal of Mechanical Engineering*, Vol. 60, No. 11, 716-724, doi:10.5545/sv-jme.2013.1588
[24] Deng, W. J.; Xie, Z. C.; Li, Q.; Lin, P. (2013). Finite element modelling and simulation of chip breaking with grooved tool, *International Journal of Simulation Modelling*, Vol. 12, No. 4, 264-275, doi:10.2507/IJSIMM12(4)5.250
[25] Gonzalez, R. C.; Woods R. E. (2002). *Digital Image Processing*, 2nd edition, Prentice Hall, Upper Saddle River
[26] Soille, P. (2004). *Morphological Image Analysis: Principles and Applications*, 2nd edition, Springer-Verlag, Berlin
[27] Ghuneim, A. G. Moore-Neighbor Tracing, from *http://www.imageprocessingplace.com/downloads_V3/root_downloads/tutorials/contour_tracing_Abeer_George_Ghuneim/moore.html*, accessed on 03-06-2015